Journal of Power Sources 196 (2011) 8822–8827

Contents lists available at ScienceDirect

Journal of Power Sources

journal homepage: www.elsevier.com/locate/jpowsour

State of charge monitoring methods for vanadium redox flow battery control

Maria Skyllas-Kazacos *, Michael Kazacos

School of Chemical Engineering, University of New South Wales, Sydney, NSW 2052, Australia

ARTICLE INFO

Article history:
Received 6 April 2011
Received in revised form 22 June 2011
Accepted 23 June 2011
Available online 29 June 2011

Keywords:
Vanadium redox battery
State-of-charge monitor
Capacity loss

ABSTRACT

During operation of redox flow batteries, differential transfer of ions and electrolyte across the membrane and gassing side reactions during charging, can lead to an imbalance between the two half-cells that results in loss of capacity. This capacity loss can be corrected by either simple remixing of the two solutions, or by chemical or electrochemical rebalancing. In order to develop automated electrolyte management systems therefore, the state-of-charge of each half-cell electrolyte needs to be known. In this study, two state-of-charge monitoring methods are investigated for use in the vanadium redox flow battery. The first method utilizes conductivity measurements to independently measure the state-of-charge of each half-cell electrolyte. The second method is based on spectrophotometric principles and uses the different colours of the charged and discharged anolyte and catholyte to monitor system balance and state-of charge of each half-cell of the VRB during operation.

1. Introduction

Redox flow batteries have many technical benefits over other energy storage systems as well as an excellent combination of energy efficiency, capital cost and life cycle costs compared with other technologies [1]. While the redox flow cell concept has been around for close to 40 years with several systems evaluated by various groups around the world, only the Vanadium Redox Flow Battery (VRB) [2–16] has to date, reached commercial fruition. The VRB was pioneered at the University of New South Wales in Australia where it was taken from the initial concept stage in 1984 through the development and demonstration of several 1–4 kW prototypes in stationary and electric vehicle applications during the late 1980s and 1990s [13,14] followed by several demonstrations and field trial by Mitsubishi Chemical Corporation and Sumitomo Electric Industries in the late 1990s to early 2000s [15,16].

The VRB has unique and highly competitive features compared to alternative battery solutions, including:

- Employs the same electrolyte solution in both half-cells, thereby eliminating cross-contamination and electrolyte maintenance problems faced by all other redox flow batteries
- Ability to scale-up the battery storage capacity at low capital cost, by simply increasing the electrolyte volume and tank size
- Indefinite life of the vanadium electrolytes reduces replacement costs and minimizes waste
- High energy efficiencies possible (up to 80%)
- Simple control and monitoring systems
- Long cycle life
- Minimal safety issues
- Can be fully discharged without harming the battery

As with all electrochemical systems however, a number of side reactions can occur during operation that can cause loss of capacity over extended charge–discharge cycling. These include:

1. Air oxidation of the V(II) ions in the negative half-cell causing an imbalance between the positive and negative electroactive species and a subsequent loss of capacity.
2. Gassing side reactions during charging – in particular hydrogen evolution at the negative electrode, leading to an imbalance between the positive and negative electroactive species and a subsequent loss of capacity.
3. Differential transfer of vanadium ions from one half-cell to the other causing a build up in one half-cell and a corresponding dilution in the other.
4. Volumetric transfer of electrolyte from one half-cell to the other due to differential pressure drop across the membrane.

While any capacity loss caused by Processes (3) and (4) can be readily corrected by simple periodic electrolyte remixing that rebalances the electrolyte compositions and liquid levels in each reservoir, capacity losses by Processes (1) and (2) can only be corrected by chemical or electrochemical rebalancing of the oxidation states of the two half-cell electrolytes. Suitable state-of-charge monitoring methods are therefore needed to detect any imbalances

* Corresponding author. Tel.: +61 2 9385 4335; fax: +61 2 9385 5966.
E-mail address: m.kazacos@unsw.edu.au (M. Skyllas-Kazacos).

0378-7753/$ – see front matter © 2011 Elsevier B.V. All rights reserved.
doi:10.1016/j.jpowsour.2011.06.080

in the individual electrolyte oxidation states so that appropriate correction procedures can be applied to restore any loss of capacity.

Traditionally, open circuit cells are used to monitor the state-of-charge of a cell by using the Nernst Equation to relate the reversible (or open-circuit potential) to the logarithm of the redox reaction ion ratio (corresponding to state-of-charge):

Although the open-circuit cell voltage (OCV) can be used as an indication of the overall cell state of charge (SOC) through the application of the Nernst equation, this will only be accurate if the system is balanced. If the electrolytes become unbalanced, however, it is not be possible to determine the electrolyte imbalance from the open-circuit voltage, nor will the cell SOC be accurately indicated by the OCV. Ideally, therefore, each of the half-cell electrolyte potentials should be monitored so that the SOC of each half-cell electrolyte can be independently monitored.

Theoretically an inert indicator electrode could be utilized in each half-cell electrolyte reservoir, however, in a large scale redox flow cell system the use of such an electrode would be impractical since solution potential measurement also requires a stable reference electrode potentia1. Reference electrodes are however inherently unreliable due to a large number of interferences that can lead to drifts in the measured potential. Furthermore, the solution potential changes only slightly over a wide range of states-of-charge so that sensitivity is poor.

Two alternative forms of SOC monitoring have thus been investigated, one which utilizes conductivity measurements and the other, absorption measurements based on spectrophotometric principles, using the different colours of the charged and discharged anolyte and catholyte to allow monitoring of system balance and state-of charge of each half-cell of the VRB during operation. In the negative half-cell of the VRB, the following colour transitions occur during charge–discharge cycling:

$$\underset{\text{violet}}{V(II)} \Leftrightarrow \underset{\text{green}}{V(III)} + e$$

while in the positive half-cell:

$$\underset{\text{yellow}}{V(V)} + e \Leftrightarrow \underset{\text{blue}}{V(IV)}$$

Electrolyte conductivity can also be used to continuously monitor state of charge and regulate charging and discharging between desired limits. Since electrolyte composition varies during charge–discharge cycling, it should be possible to monitor individual half-cell solution conductivities and correlate these to the SOC or oxidation state of each half-cell.

2. Experimental

In this study, vanadium solutions of compositions corresponding to different negative and positive half-cell electrolyte states-of-charge, were prepared by the electrolysis of 2 M vanadyl sulfate solutions in different concentrations of H_2SO_4 supporting electrolyte. The vanadyl sulfate stock solution was placed into both halves of an electrolysis cell (with twice the volume used on the positive side) and electrolysed at a current density of 20 mA cm^{-2} to produce 2 M V(V) in the positive half-cell and 2 M V(II) in the negative.

During electrolysis, the following reactions take place:

In the positive half-cell:

$$VO^{2+} + H_2O \rightarrow VO_2^{+} + 2H^{+} + e \quad (1)$$

In the negative half-cell:

$$VO^{2+} + 2H^{+} + e \rightarrow V^{3+} + H_2O \quad (2)$$

followed by:

$$V^{3+} + e \rightarrow V^{2+} \quad (3)$$

The end-point in the electrolysis was taken as the time when the positive and negative electrolytes turned yellow and violet respectively, verifying that the solutions were close to 100% V(V) and V(II).

A portion of each of the 2 solutions was removed from the cell and the remaining volumes were then pumped through the cell to allow the discharge reactions to occur to produce a green V(III) solution in the negative half-cell and a blue V(IV) solution in the positive.

The resultant solutions were mixed in different V(II):V(III) and V(V):V(IV) ratios to simulate a range of electrolyte states of charge. Solutions of different vanadium and total sulfate concentrations were prepared with this method and used for the conductivity and UV–vis spectroscopic measurements.

The UV–vis spectra of the vanadium solutions were measured using a Varian Superscan 3 double beam spectrophotometer with a scan rate of 200 nm min^{-1}.

Conductivities were measured with a Type CDM2e Radiometer conductivity meter with a Type CD104 Radiometer conductivity probe. The apparatus was calibrated using a 0.05% NaCl solution and the probe was allowed to equilibrate for 5 min or until steady state was reached.

3. Results and discussion

3.1. Electrolyte conductivity as a function of state-of-charge

The conductivities of V(V), V(IV), V(III) and V(II) solutions were measured for different vanadium and total sulfate concentrations using a Radiometer CDM2e conductivity meter and the results are presented in Table 1 for a temperature of 22 ± 1 °C.

From the results summarized in Table 1, it can be seen that of all the vanadium ions, V(V) has the highest conductivity in H_2SO_4 solutions. This is mainly due to the higher proton concentration in the V(V) solution compared with the corresponding V(IV), V(III) and

Table 1
Effect of composition on conductivity. Temperature = 22° ± 1° C.

Vanadium ion	Vanadium ion concentration (M) ±0.1 M	Total sulfate concentration (M) ±0.1 M	Conductivity (mS cm^{-1}) ±5%
V(V)	2.0	5.0	365
	2.0	4.5	350
	2.0	4.0	335
	1.5	4.0	385
	1.0	4.0	420
	0.5	4.0	440
V(IV)	2.0	5.0	200
	2.0	4.5	200
	2.0	4.0	175
	1.5	4.0	229
	1.0	4.0	285
	0.5	4.0	340
V(III)	2.0	5.0	220
	2.0	4.5	190
	2.0	4.0	160
	1.5	4.0	210
	1.0	4.0	270
	0.5	4.0	339
V(II)	2.0	5.0	240
	2.0	4.5	230
	2.0	4.0	210
	1.5	4.0	260
	1.0	4.0	320
	0.5	4.0	370

V(II) solutions. As seen from Eqs. (1) and (2), the oxidation of V(IV) to V(V) produces protons, while the reduction to V(III) consumes protons, causing the conductivity to increase in the case of V(V) and decrease in the case of the V(III) and V(II) solutions.

Ion-pairing interactions between SO_4^{2-} and the VO^{2+} and VO_2^+ ions [17] will also affect the free proton concentration and thereby further enhance the conductivity as illustrated by Eqs. (4)–(7):

$$VO^{2+} + SO_4^{2-} \Leftrightarrow VO^{2+} \cdots SO_4^{2-} \quad (4)$$

$$VO_2^+ + SO_4^{2-} \Leftrightarrow VO_2^+ \cdots SO_4^{2-} \quad (5)$$

These ion pairing interactions (Eqs. (4) and (5)), will cause the acid dissociation equilibria (Eqs. (6) and (7)) to shift to the right, increasing the free H^+ concentration in the V(IV) and V(V) solutions, further increasing the conductivity of the positive half-cell electrolyte.

$$H_2SO_4 \Leftrightarrow H^+ + HSO_4^- \quad K = 2.4 \times 10^6 \quad (6)$$

$$HSO_4^- \Leftrightarrow H^+ + SO_4^{2-} \quad K = 1 \times 10^{-2} \quad (7)$$

Of the above acid dissociation equilibria, the first dissociation is essentially complete, while the second dissociation does not occur to any significant extent. As sulfate ions are consumed by the V(IV) and V(V) ion pairing reactions (Eqs. (4) and (5)) however, the second acid dissociation equilibrium (Eq. (7)) shifts to the right, releasing additional protons that increase the conductivity of the solution.

The conductivity values in Table 1 also show that as the vanadium concentration is increased, the electrolyte conductivity decreases for each of the vanadium oxidation states. This is again due to a shift in the acid dissociation equilibria. As more vanadium sulfate is added to the solution, the increase in the SO_4^{2-} concentration causes equilibrium [7] to shift towards the left reducing the free proton concentration and thereby reducing conductivity:

Of course a high vanadium concentration is desirable for higher energy densities, but as shown by these results, this can only be achieved, at the expense of electrolyte conductivity and higher iR losses in the cell.

For increased conductivity therefore, 2 M vanadium in 5 M total sulfates is often selected as the preferred electrolyte composition for the VRB. This electrolyte composition was thus chosen for further study of the trends in conductivity with state of charge and Figs. 1 and 2 presents the results obtained for the negative and positive electrolytes respectively at 3 different temperatures. Some slight scatter in the data is observed at different temperatures due to experimental error with the conductivity probe and slight fluctuations in the set temperature during measurement. Also, some discrepancies between the conductivity values at 22 °C in Table 1 and the data at 20 °C in Figs. 1 and 2, are due to slight variations in solution composition between batches, this being due to water losses and gassing reactions during solution preparation by electrolysis that are very difficult to control. Attempts to adjust the composition after electrolysis proved difficult because of the limited accuracy (±5%) of the potentiometric titration and atomic spectroscopic techniques used to determine total vanadium concentration.

Despite these limitations, however, definite trends in conductivity are seen with both SOC and temperature. As expected, conductivity increases with increasing temperature, and in both the positive and negative half-cell electrolytes, a linear increase is observed with increasing SOC, although a slight deviation is seen in the negative half-cell electrolyte at high SOCs. This is believed to be due to air oxidation of the V(II) ions at higher temperatures during the conductivity measurements, giving rise to lower than expected conductivity values for the corresponding SOC. These trends in conductivity can be explained as follows.

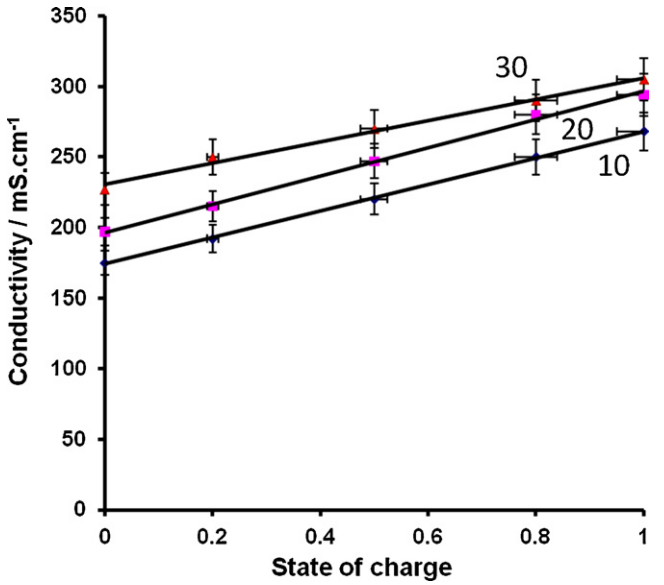

Fig. 1. Plot of conductivity of negative vanadium cell electrolyte as a function of state-of-charge (2 M V in 5 M total sulfate) for temperatures of 30 ± 1, 20 ± 1 and 10 ± 1 °C.

During the charging reaction in the positive half-cell, given by Eq. (1), two hydrogen ions are produced by every oxidized VO^{2+} ion and one electron is transferred from the positive electrode to the negative. For charge neutrality, one hydrogen ion will also be transferred across the membrane into the negative half-cell leading to a net increase of one proton per vanadium ion reacted in each half cell electrolyte. With increasing SOC therefore, the hydrogen ion concentration will gradually increase in both half-cells, giving rise to an increase in conductivity. This linear relationship between conductivity and SOC can therefore be used in the development of an SOC monitoring system.

In this study, conductivity values were determined for a 2 M vanadium solution in 5 M total sulfates at 3 different temperatures. These measurements can be used to determine temperature coefficients for temperature compensation of conductivity values for this specific electrolyte composition. The composition of the VRB electrolyte (both in terms of the total vanadium and total sulfate

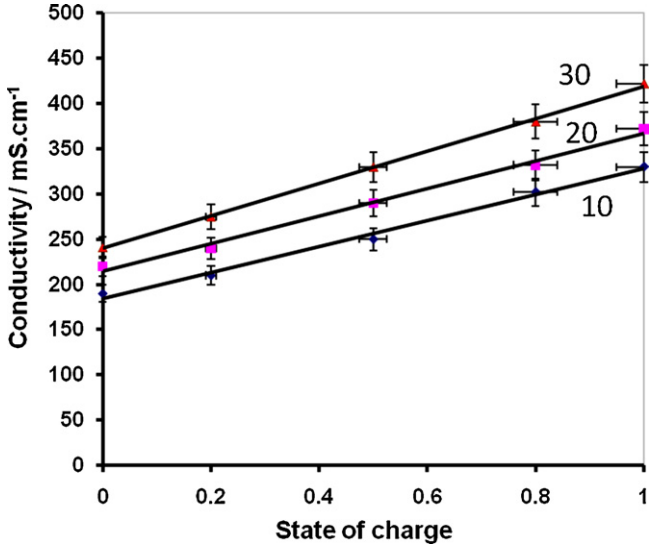

Fig. 2. Plot of conductivity of a positive electrolyte (2 M V in 5 M total sulfate) as a function of state-of-charge for temperatures of 30 ± 1, 20 ± 1 and 10 ± 1 °C.

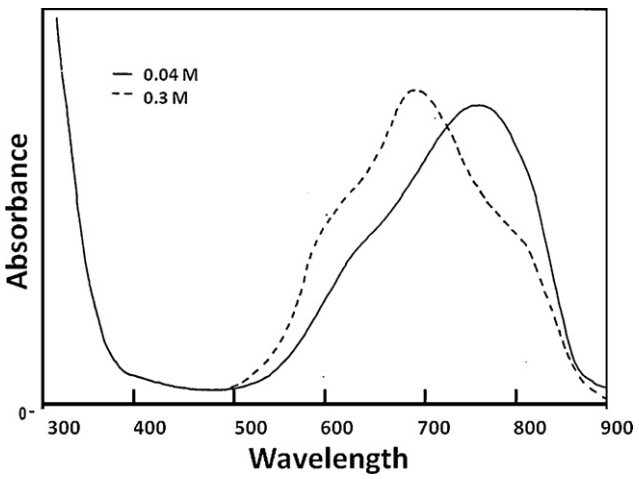

Fig. 3. UV–vis spectrum for 0.04 M and 0.3 M $VOSO_4$ in 2 M H_2SO_4 [19].

concentration) is often adjusted to suit different climates and operational conditions however, so calibration of the conductivity vs SOC plots would be needed for the specific electrolyte composition used.

Although the present focus has been on the use of conductivity measurements for SOC monitoring in the VRB, this approach could be readily applied in other types of electrochemical cells or reactors. All membrane-based electrochemical cells involve the transfer of protons or other ions from one half-cell to the other for charge neutrality. In all flow batteries therefore, this phenomenon will produce changes in electrolyte conductivities during charge–discharge cycling that can be monitored and used for SOC monitoring. The same approach can therefore be applied to all other redox flow cell chemistries for the purpose of monitoring individual cell SOCs for capacity correction during long-term operation.

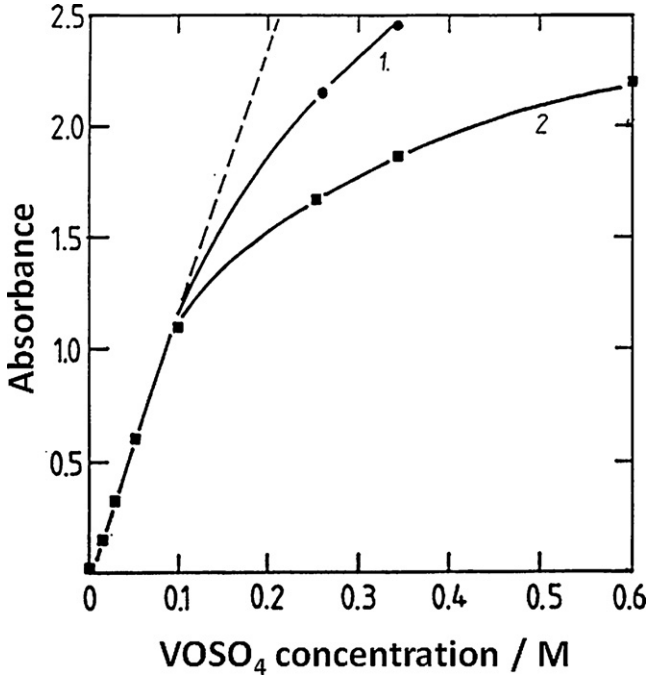

Fig. 4. Beer's Law plot for V(IV) in 2 M sulfuric acid supporting electrolyte at (1) maximum absorbance wavelength in the range 700–760 nm, and (2) wavelength of 750 nm.

3.2. Spectrophotometric studies of electrolytes as a function of state-of-charge

As described above, the vanadium electrolytes undergo distinctive colour changes during charging and discharging of the vanadium battery. The colours corresponding to each oxidation state are, V(II) (violet), V(III) (green) and V(IV) (blue), V(V) (yellow), with different shades of green and turquoise in between. Given these distinctive colour changes during charging and discharging of the VRB, the use of spectrophotometric methods for state-of-charge (SOC) monitoring was proposed by Skyllas-Kazacos et al. [18].

Grossmith et al. [19] measured the absorbance for a series of V(IV) solutions to establish whether Beer's Law is obeyed (i.e. whether absorbance was directly proportional to concentration). Fig. 3 shows a UV–vis spectrum for 0.04 M and 0.3 M VOSO, in 2 M H_2SO_4. A Beer's Law plot is given in Fig. 4, and shows that Beer's Law is obeyed for absorbances less than 1.0, corresponding to a $VOSO_4$ concentration of approximately 0.1 M. The very rapid deviation above this concentration was shown to be largely due to the changing peak position.

From Beer's Law, absorbance is a function of both concentration and path length:

$$A = abc \tag{8}$$

where A = absorbance; a = molar absorptivity; b = path length; c = molar concentration.

For absorbances less than 1 therefore, either concentration or path length could be reduced. In practical VRB systems however, the use of dilute vanadium solutions for SOC monitoring would be impractical, as would the use of very small tube diameters for electrolyte flow. The possibility of using absorbance measurements at wavelengths other than the peak absorbance was therefore considered.

A series of spectrograms for 2 M V(V)/V(IV) solutions representing different SOCs of the positive electrolyte (e.g. curve 1 = 100% SOC and curve 10 = 0% SOC) is shown in Fig. 5. As can be seen, over the majority of the SOC range (95–10%) the absorption is too high within the UV–vis range to permit measurement in the 1 cm cuvette. The use of absorbance for SOC monitoring of the positive half-cell electrolyte is therefore not feasible.

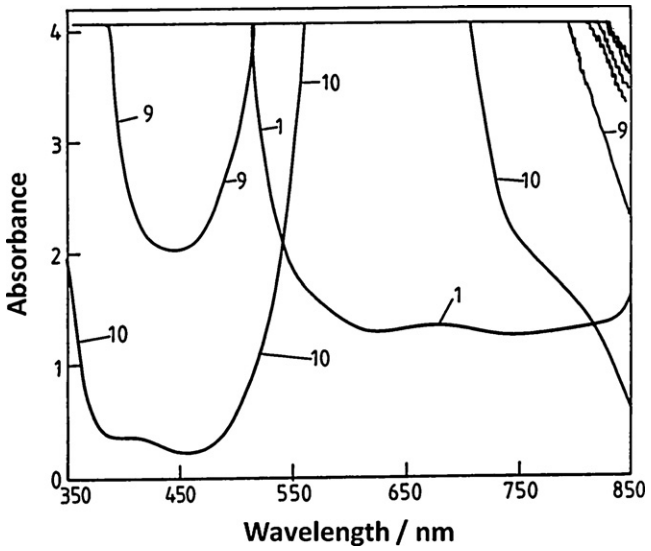

Fig. 5. UV–vis spectra for 2 M positive electrolytes at different states-of-charge. Curves 1–10 correspond to state-of-charge values of 1.0, 0.95, 0.90, 0.80, 0.60, 0.40, 0.20, 0.10, 0.05 and 0, respectively.

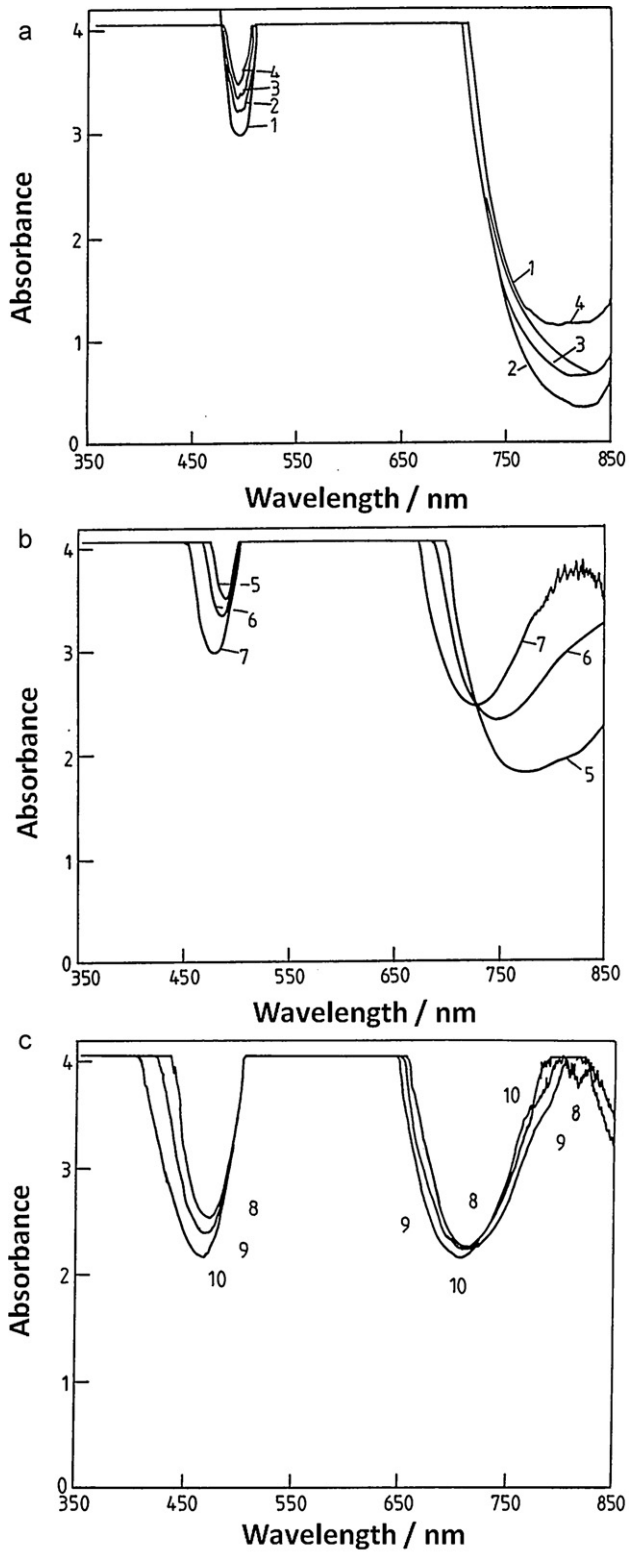

Fig. 6. (a) UV–vis spectra for 2 molar vanadium negative electrolytes at different states-of-charge. Curves 1–4 correspond to SOC values 1.0, 0.95, 0.9 and 0.8, respectively. (b) UV–vis spectra for 2 molar vanadium negative electrolytes at different states-of-charge. Curves 5–7 correspond to SOC values of 0.6, 0.4, and 0.2, respectively. (c) UV–vis spectra for 2 molar vanadium negative electrolytes at different states-of-charge. Curves 8–10 correspond to SOC values 0.1, 0.5 and 0, respectively.

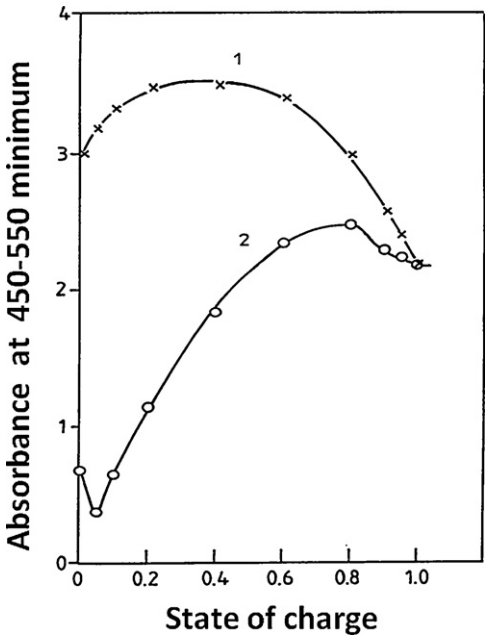

Fig. 7. Plot of absorbance of 2 molar vanadium negative electrolyte as a function of SOC. Curve 1 corresponds to absorbance at the minimum in the spectrum in the at 450–500 nm range, curve 2 is absorbance at the 300–850 nm minimum.

In the case of the negative half-cell electrolyte however, 2 minima with absorbances close to or less than one are observed in the absorption curves, as shown in Fig. 6. The position of the two minima, varies as a function of composition, however, plotting the absorbance of the solutions as a function of SOC at the 2 minima in the spectrum at 450–500 nm and at 700–850 nm, gives rise to curves 1 and 2, respectively in Fig. 7. If the absorbance of the solutions is plotted as a function of SOC at 750 nm however, a linear relationship is obtained over the range 5% to 100% SOC as shown in Fig. 8.

This linear relationship could therefore be used in the development of a simple SOC monitor for the negative half-cell electrolyte.

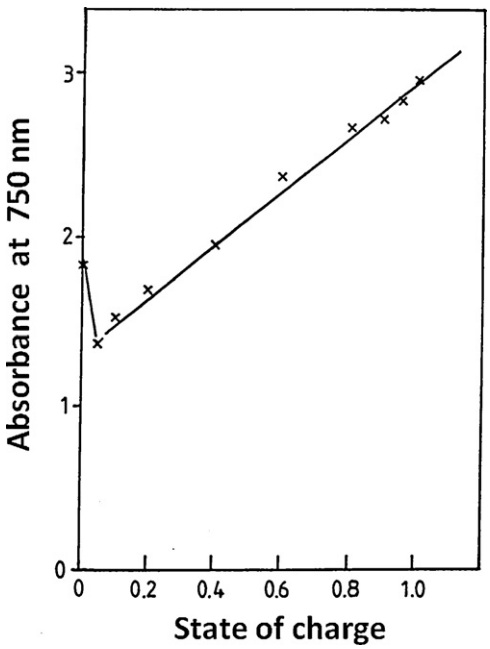

Fig. 8. Plot of absorbance of 2 molar vanadium negative electrolyte at 750 nm as a function of state-of-charge.

An SOC sensor based on solution absorbance will therefore allow easy monitoring of any deviations in the negative electrolyte SOC relative to the total cell state-of-charge caused by air oxidation of V(II) or hydrogen evolution at the negative electrode during charging. As with conductivity measurements however, absorbance is a function of electrolyte composition and temperature, so calibration of the specific electrolyte composition used in the VRB system would be required. Furthermore, during charge–discharge cycling, changes in solution temperature will affect solution absorbance due to shifts in the ionic equilibria. More detailed analysis of temperature effects on solution absorbance would therefore need to be undertaken to correct for temperature effects that would lead to errors in calculated SOC values.

Although the present study has focused on the development of SOC monitoring methods for VRB electrolytes, most of the redox couples used in other types redox flow batteries also exhibit distinct colours for each of the ion oxidation states (e.g. Fe(II)/Fe(III), Br^-/Br_2, Ce(III)/Ce(IV) etc.). Solution absorbance can therefore be readily applied for SOC monitoring of other redox battery systems as well [20]. Simple calibration of a range of solution properties as a function of state-of-charge can thus lead to the development of simple sensors for a range of redox flow cell technologies.

4. Conclusions

Two techniques are investigated for the individual state-of-charge monitoring of the two half-cell electrolytes of the vanadium redox flow battery. The first technique uses the linear variation in electrolyte conductivity with SOC, while the second uses light absorption to take advantage of the solution colour changes during charging and discharging of the VRB. Although the latter approach is not viable for the positive half-cell solution due to its very high absorbance over most of the UV–vis range, a linear relationship in absorbance of the negative half-cell electrolyte vs SOC is identified at a wavelength of 750 nm. A simple detector can thus be used to monitor the absorbance by the solution of 750 nm radiation passing through a flat-sided tube through which the negative electrolyte is recirculated into and out of the battery stack. The absorbance measurement is easily converted into an SOC value for the negative half-cell solution. This can be compared to the overall cell SOC obtained from OCV measurements to determine the extent of electrolyte imbalance that leads to capacity loss during operation of the VRB. As with conductivity measurements however, absorbance is a function of electrolyte composition, so calibration of the specific electrolyte composition used in the VRB system allows easy monitoring of any deviations in the negative electrolyte SOC relative to the total cell state-of-charge caused by any gassing side reactions during charging and/or air oxidation of V(II) in the negative half-cell electrolyte tanks. The poor correlation for the positive half-cell electrolyte absorbance with SOC is a limiting factor in the use of this method for determining electrolyte imbalances in the VRB however, particularly those arising from Processes (3) and (4), although other redox flow cell chemistries could prove more amenable to this approach.

Various SOC sensors using OCV, absorbance and conductivity measurements can thus be incorporated into sophisticated electrolyte management systems for flow batteries that can be used to schedule electrolyte rebalancing procedures such as periodic remixing or chemical/electrochemical rebalancing that allow any reduction in capacity over long-term operation to be fully restored.

References

[1] Electricity Storage Association website: http://www.electricitystorage.org/ESA/technologies/vanadium_redox_batteries/ (accessed 05.07.10).
[2] M. Skyllas-Kazacos, R.G. Robins, All-vanadium redox battery, US Pat. 4,786,567, 1986.
[3] M. Skyllas-Kazacos, M. Rychcik, R.G. Robins, A.G. Fane, M. Green, J. Electrochem. Soc. 133 (1986) 1057–1058.
[4] M. Skyllas-Kazaocs, M. Rychcik, J. Power Sources 19 (1987) 45–54.
[5] B.T. Sun, M. Skyllas-Kazacos, Electrochim. Acta 37 (1992) 1253–1269.
[6] M. Kazacos, M. Cheng, M. Skyllas-Kazacos, J. Appl. Electrochem. 20 (1990) 463–467.
[7] T. Mohammadi, M. Skyllas-Kazacos, J. Power Sources 56 (1995) 91–96.
[8] T. Mohammadi, M. Skyllas-Kazacos, J. Appl. Electrochem. 27 (1996) 153–160.
[9] T. Sukkar, M. Skyllas-Kazacos, J. Membr. Sci. 222 (2003) 235–247.
[10] M. Kazacos, M. Skyllas-Kazacos, J. Electrochem. Soc. 136 (1989) 2759–2760.
[11] V. Haddadi-Asl, M. Kazacos, M. Skyllas-Kazacos, J. Appl. Polym. Sci. 57 (1995) 1455–1463.
[12] M. Skyllas-Kazacos, D. Kasherman, R. Hong, M. Kazacos, J. Power Sources 35 (1991) 399–404.
[13] R. Largent, M. Skyllas-Kazacos, J. Chieng, Proceedings IEEE, 23rd Photovoltaic Specialists Conference, Louisville, Kentucky, May 1993.
[14] C. Menictas, D.R. Hong, Z.H. Yan, J. Wilson, M. Kazacos, M. Skyllas-Kazacos, Proceedings, Electrical Engineering Congress, Sydney, November 1994.
[15] N. Tokuda, T. Kumamoto, T. Shigematsu, H. Deguchi, T. Ito, N. Yoshikawa, T. Hara, SEI Tech. Rev. 45 (January) (1998).
[16] N. Tokuda, T. Kanno, T. Hara, T. Shigematsu, Y. Tsustui, A. Ikeuchi, T. Itou, T. Kumamoto, SEI Tech. Rev. 50 (June) (2000) 88–94.
[17] A.A. Ivakin, E.M. Voronova, Russ. J. Inorg. Chem. 18 (1973) 956.
[18] M. Skyllas-Kazacos, M. Kazacos, J. Joy, B.G. Madden, "State-of-Charge of Redox Cell", Patent Appl. No. PCT/AU89/00252, June 1989.
[19] F. Grossmith, P. Llewellyn, A. Fane, M. Skyllas-Kazacos, in: Proceedings of Symposium on Energy Storage: Load Levelling and Remote Applications, Electrochem. Soc. Proceedings, Electrochem. Soc. 88 (11) (1988).
[20] S.K. Sahu, Apparatus and Methods of Determination of State of Charge in a Redox Flow Battery, US 7855005 B2, Dec., 2010.